Brushes of flexible, semiflexible, and rodlike diblock polyampholytes: Molecular dynamics simulation and scaling analysis

Majid Baratlo and Hossein Fazli*
Institute for Advanced Studies in Basic Sciences, Zanjan 45195-1159, Iran
(Received 30 September 2009; revised manuscript received 24 November 2009; published 5 January 2010)

Planar brushes of flexible, semiflexible, and rodlike diblock polyampholytes are studied using molecular dynamics simulations in a wide range of the grafting density. Simulations show linear dependence of the average thickness on the grafting density in all cases regardless of different flexibility of anchored chains and the brushes' different equilibrium conformations. Slopes of fitted lines to the average thickness of the brushes of semiflexible and rodlike polyampholytes versus the grafting density are approximately the same and differ considerably from that of the brushes of flexible chains. The average thickness of the brush of flexible diblock polyampholytes as a function of the grafting density is also obtained using a simple scaling analysis, which is in good agreement with our simulations.

DOI: 10.1103/PhysRevE.81.011801 PACS number(s): 82.35.Rs, 61.41.+e, 87.15.−v

I. INTRODUCTION

Macromolecules containing ionizable groups when dissolve in a polar solvent such as water, dissociate into charged macromolecules and counterions (ions of opposite charge). Depending on acidic or basic property of their monomers, ionizable polymers in solution can be classified into polyelectrolytes and polyampholytes. Polyelectrolytes contain a single sign of charged monomers and polyampholytes bear charged monomers of both signs. These macromolecules are often water soluble and have numerous industrial and medical applications. Many biological macromolecules such as DNA, RNA, and proteins are charged polymers. In polymer science, charged polymers has been an important subject during last several decades [1–4]. Contrary to a polyelectrolyte chain, in which the intrachain electrostatic interactions are repulsive and tend to swell the chain, in a polyampholyte chain attractive interactions between charged monomers of opposite sign tend to decrease the chain size. Oppositely charged monomers can be distributed randomly along a polyampholyte chain or charges of one sign can be arranged in long blocks. With the same ratio of positively and negatively charged monomers (isoelectric condition), behaviors of a single polyampholyte and the solution of polyampholytes depend noticeably on the sequence of charged monomers on the chains. For example, it has been shown that the sequence of charged amino acids (charge distribution) along ionically complementary peptides affect the aggregation behavior and self-assembling process in the solution of such peptides [5,6]. Also, using Monte Carlo simulations it has been shown that charged monomers sequence of charge-symmetric polyampholytes affect their adsorption properties to a charged surface [7].

The properties of the system of polymers anchored on a surface are of great interest both in industrial and biological applications and academic research. With a sufficiently strong repulsion between the polymers, the chains become stretched and the structure obtained is known as a polymer brush. Planar and curved brushes formed by grafted homopolymers have extensively been investigated by various theoretical methods [8–11].

The anchored polymers of a brush may be consisting of charged monomers. In this case, the brush is known as a polyelectrolyte or a polyampholyte brush depending on the charged monomers of the chains being of the same sign or being composed of both signs. In a brush of charged polymers, electrostatic interactions introduce additional length scales such as Bjerrum length and Debye screening length to the system.

In a polyelectrolyte brush, the repulsion of electrostatic origin between the chains can be sufficiently strong even at low grafting densities, making it easy for the system to access the brush regime. Polyelectrolyte brushes have been investigated extensively using both theoretical [12–19] and computer simulation methods [17–22]. At high enough grafting densities and charge fractions of polyelectrolyte chains, most of counterions are trapped inside the polyelectrolyte brush and competition between osmotic pressure of the counterions and elasticity of the chains determines the brush thickness. This regime of a polyelectrolyte brush is known as the osmotic regime in which some theoretical scaling methods predict no dependence of the brush thickness to the grafting density [12,23]. However, other scaling method that takes into account the excluded volume effects and nonlinear elasticity of polyelectrolyte chains and is in agreement with experiment and simulation, predicts a linear dependence of the brush thickness on the grafting density [17–19]. Also, it has been shown that diffusion of a fraction of counterions outside the polyelectrolyte brush leads to a logarithmic dependence of the average brush thickness on the grafting density [16].

Electrostatic interactions in a polyelectrolyte brush cause most of the counterions to be trapped inside the brush and help the chains to be more stretched and the brush to be more aligned. However, in a brush of overall neutral polyampholyte chains, most of counterions are outside the brush and the electrostatic correlations tend to decrease the chains size and the brush thickness. At a given value of the grafting density, the average thickness and equilibrium properties of

*fazli@iasbs.ac.ir

such a polyampholyte brush are mainly determined by the chains properties such as fraction and sequence of charged monomers and the bending energy. Brushes formed by grafted diblock polyampholytes have been investigated by lattice mean field modeling [24,25] and computer simulation [26]. The effect of chain stiffness, charge density and grafting density on spherical brushes of diblock polyampholytes and interaction between colloids with grafted diblock polyampholytes have been studied using Monte Carlo simulations [27,28]. Also, using molecular dynamics (MD) simulations, the effects of various parameters such as charged monomers sequence, grafting density and salt concentration on the average thickness and equilibrium conformations of planar semiflexible polyampholyte brushes have been investigated [29].

In this paper, we study planar brushes of flexible, semiflexible, and rodlike diblock polyampholytes using MD simulations in a wide range of the grafting density. We find that in all cases the average brush thickness linearly depends on the grafting density regardless of the chains different flexibility. Our results also show that the strength of this dependence is considerably weaker in the case of the brush of flexible polyampholytes than two other cases. Despite mentioned same functionality obtained for the average thickness versus the grafting density for brushes of different polyampholytes we find that histograms of their equilibrium conformations are noticeably different. Interchain correlations are too weak in the brush of flexible polyampholytes and the brush properties are dominantly determined by single chain behavior. In this case, dependence of the equilibrium conformation of the brush on the grafting density is very weak. In the cases of the brushes of semiflexible and rodlike polyampholytes however, because of the combination of electrostatic correlations and strong excluded volume effects, collective behavior of the chains is dominant and dependence of equilibrium conformations on the grafting density is strong. In these cases, we also observe separation of the anchored chains into two coexisting fractions. Using a simple scaling method which is consistently applicable for the brush of flexible chains, we describe theoretically the linear dependence of the brush thickness on the grafting density.

The rest of the paper is organized as follows. In Sec. II, we describe our model and simulation method in detail and present the results of MD simulations. Our scaling analysis to describe dependence of the average thickness of flexible diblock polyampholyte brushes on the grafting density is presented in Sec. III. In Sec. IV, we conclude the paper and present a short discussion.

II. MOLECULAR DYNAMICS SIMULATION OF DIBLOCK POLYAMPHOLYTE BRUSHES

A. Model and the simulation details

In our simulations which are performed with the MD simulation package ESPRESSO [30], each brush is modeled by $M=25$ diblock polyampholyte bead-spring chains of length $N=24$ (24 spherical monomers), which are end-grafted onto an uncharged surface at $z=0$. The positions of anchored monomers which are fixed during the simulation, form a square lattice on the grafting surface ($x-y$ plane) with lattice spacing $d=\rho_a^{-1/2}$, in which ρ_a is the grafting density of the chains. The fraction $f=\frac{1}{2}$ of the monomers of each chain are charged and the chains consist of an alternating sequence of charged and neutral monomers. Each chain contains the same number of positively and negatively charged monomers with charges e and $-e$ respectively (see Fig. 1). Excluded volume interaction between particles is modeled by a shifted Lennard-Jones potential,

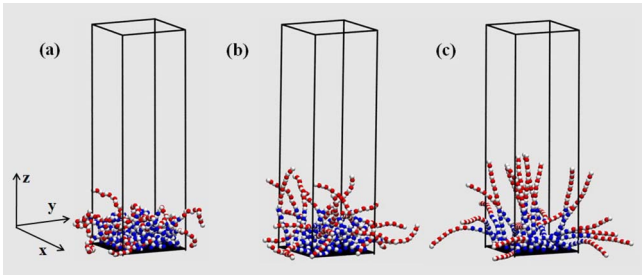

FIG. 1. (Color online) Sample snapshots of brushes of (a) flexible ($l_p=5\sigma$), (b) semiflexible ($l_p=25\sigma$), and (c) rodlike ($l_p=200\sigma$) diblock polyampholytes at grafting density $\rho_a\sigma^2=0.08$. Neutral, positively, and negatively charged monomers are shown by white, red (dark), and blue (black) spheres, respectively (see also Fig. 5). Counterions are not shown and periodic boundary condition is removed for clarity.

$$u_{LJ}(r)=\begin{cases}4\varepsilon\left\{\left(\frac{\sigma}{r}\right)^{12}-\left(\frac{\sigma}{r}\right)^{6}+\frac{1}{4}\right\} & \text{if } r<r_c,\\ 0 & \text{if } r\geq r_c,\end{cases} \quad (1)$$

in which ϵ and σ are the usual Lennard-Jones parameters and the cutoff radius is $r_c=2^{1/6}\sigma$. Successive monomers of each chain are bonded to each other by a finite extensible nonlinear elastic (FENE) potential [31],

$$u_{bond}(r)=\begin{cases}-\frac{1}{2}k_{bond}R_0^2\ln\left[1-\left(\frac{r}{R_0}\right)^2\right] & \text{if } r<R_0\\ 0 & \text{if } r\geq R_0,\end{cases} \quad (2)$$

with bond strength $k_{bond}=30\varepsilon/\sigma^2$ and maximum bond length $R_0=1.5\sigma$. Bending elasticity of the chains is modeled by a bond angle potential,

$$u_{bend}(r)=k_{bend}(1-\cos\theta), \quad (3)$$

in which θ is the angle between two successive bond vectors and k_{bend} is the bending energy of the chains. The value of the persistence length, l_p, of the chains depends on the value of k_{bend} as $l_p=\frac{k_{bend}}{k_BT}\sigma$. To model brushes of flexible, semiflexible, and rodlike chains, we use four different values of k_{bend}, namely, 0, $5k_BT$, $25k_BT$, and $200k_BT$, respectively. The simulation box is of volume $L\times L\times L_z$, in which L is the box width in x and y directions and L_z is its height in z direction and the grafting density is given by $\rho_a=M/L^2$. We consider $M\times N\times f$ monovalent counterions to neutralize the chains charge. Positive and negative monovalent counterions are modeled by equal number of spherical Lennard-Jones particles of diameter σ with charges e and $-e$, respectively. All

the particles interact repulsively with the grafting surface at short distances with the shifted Lennard-Jones potential introduced in Eq. (1). In addition, a similar repulsive potential is applied at the top boundary of the simulation box and in our simulations $L_z=2N\sigma$. All the charged particles interact with each other with the Coulomb interaction

$$u_C(r) = k_B T q_i q_j \frac{l_B}{r}, \tag{4}$$

in which q_i and q_j are charges of particles i and j in units of elementary charge e and r is separation between them. The Bjerrum length, l_B, which determines the strength of the Coulomb interaction relative to the thermal energy, k_BT, is given by $l_B=e^2/\varepsilon k_BT$, where ε is the dielectric constant of the solvent and we set $l_B=2\sigma$ in our simulations. Periodic boundary conditions are applied only in two dimensions (x and y). To calculate Coulomb forces and energies, we use the so-called *MMM* technique introduced by Strebel and Sperb [32] and modified for laterally periodic systems (*MMM2D*) by Arnold and Holm [33]. The temperature in our simulations is kept fixed at $k_BT=1.2\varepsilon$ using a Langevin thermostat.

For each value of the bending energy, k_{bend}, we do simulations of the brush at dimensionless grafting densities $\rho_a\sigma^2=0.02$, 0.04, 0.06, 0.08, and 0.10. In the beginning of each simulation, all of the chains are straight and perpendicular to the grafting surface and all the ions are randomly distributed inside the simulation box. We equilibrate the system for 1.6×10^6 MD time steps which is enough for all values of the grafting density mentioned above and then calculate thermal averages over 1500 independent configurations of the system selected from 2.25×10^6 additional MD steps after equilibration. MD time step in our simulations is $\tau=0.01\tau_0$, in which $\tau_0=\sqrt{\frac{m\sigma^2}{\varepsilon}}$ is the MD time scale and m is the mass of the particles.

We calculate the average brush thickness which can be measured by taking the first moment of the monomer density profile,

$$\langle z_m \rangle = \frac{\int_0^\infty z\rho_m(z)dz}{\int_0^\infty \rho_m(z)dz}, \tag{5}$$

in which $\rho_m(z)$ is the number density of monomers as a function of the distance from the grafting surface. For a better monitoring of the statistics of the chains conformations, we calculate the histogram of the mean end-to-end distance of the chains, $P(R)$, in which $R=\frac{1}{M}\Sigma_{i=1}^{M}|\mathbf{R}_i|$ and $\mathbf{R}_i$ is the end-to-end vector of chain i. We also calculate the histogram of the average distance of the end monomers of the chains from the grafting surface, $P(z_{end})$, in which $z_{end}=\frac{1}{M}\Sigma_{i=1}^{M}z_i$ and z_i is the z component of the end monomer of chain i. With the same method discussed in [29], it has been checked that our results are not affected by finite-size effects (see Sec. IV).

B. Results

The average thickness versus the grafting density for brushes of flexible, semiflexible, and rodlike diblock polyampholytes are shown in Fig. 2. Dependence of the average thickness on the grafting density can be described well by a linear function for all values of the bending energy, k_{bend}, that we use in our simulations. Also, it can be seen that at all values of the grafting density the average brush thickness decreases with increasing the flexibility of the chains. Linear fits to the average thickness of the brushes of semiflexible and rodlike chains for which the persistence length, l_p, exceeds their contour length, L_c, are of approximately the same slope (see solid and dashed lines in Fig. 2). The slopes of the linear dependence in cases of two brushes of flexible chains are also approximately the same and differ by a factor of $\sim\frac{1}{2}$ from those of two other cases (dotted and dash-dotted lines in Fig. 2). To analyze such dependencies of the brushes thickness on the grafting density, we look at the equilibrium conformations statistics of the chains at different values of ρ_a. In Figs. 3 and 4 the histograms $P(R)$ and $P(z_{end})$ at three different grafting densities are shown for brushes of flexible, semiflexible, and rodlike chains. Because of very similar behaviors of the histograms in $k_{bend}=0$ and $k_{bend}=5k_BT$ cases, the histograms of the brush with $k_{bend}=0$ are not shown for clarity of the figures. As it can be seen in Fig. 3, in the case of the brush of flexible diblock polyampholytes ($k_{bend}=5k_BT$), dependence of the histogram profile on the grafting density is very weak. Also, in this case, the contribution of large values of r ($r\simeq L_c$) in the histogram is negligible, which shows that the chains are mostly coiled at all grafting densities [see a sample configuration of the brush at $\rho_a\sigma^2=0.08$ in Fig. 1(a)]. In the case of the brush of semiflexible chains ($k_{bend}=25k_BT$), with increasing the grafting density, the values of the histogram corresponding to smaller values of r become nonzero showing that polyampholyte chains take buckled conformations at high grafting densities [29]. As it is expected, the histogram $P(R)$ of the brush of rodlike chains ($k_{bend}=200k_BT$) exhibit no noticeable buckling of the

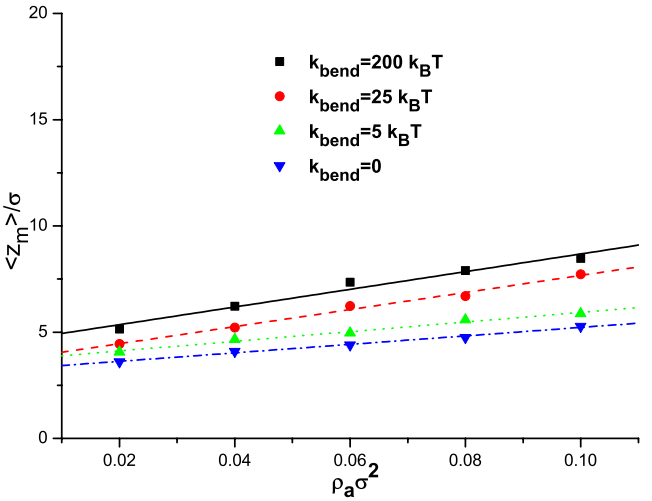

FIG. 2. (Color online) The average thickness of the brushes formed by flexible ($k_{bend}=0$ and $5k_BT$), semiflexible ($k_{bend}=25k_BT$), and rodlike ($k_{bend}=200k_BT$) diblock polyampholytes versus dimensionless grafting density, $\rho_a\sigma^2$. The lines are linear fits to our simulation data. The slopes of solid, dashed, dotted and dash-dotted lines are 41.6, 40.2 and 22.7 and 20.0, respectively. The size of the symbols corresponds to the size of error bars.

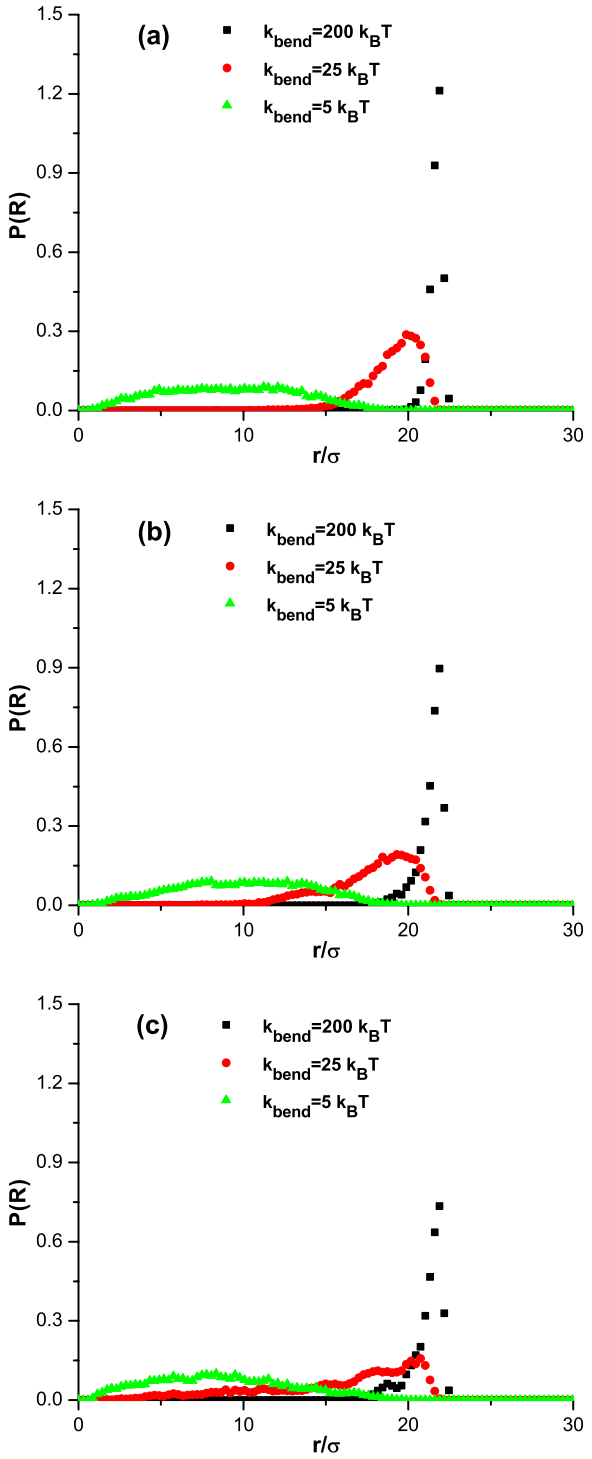

FIG. 3. (Color online) Histogram of the average end-to-end distance of the chains for brushes formed by flexible, semiflexible, and rodlike diblock polyampholytes at grafting densities (a) $\rho_a\sigma^2=0.02$, (b) $\rho_a\sigma^2=0.06$, and (c) $\rho_a\sigma^2=0.10$.

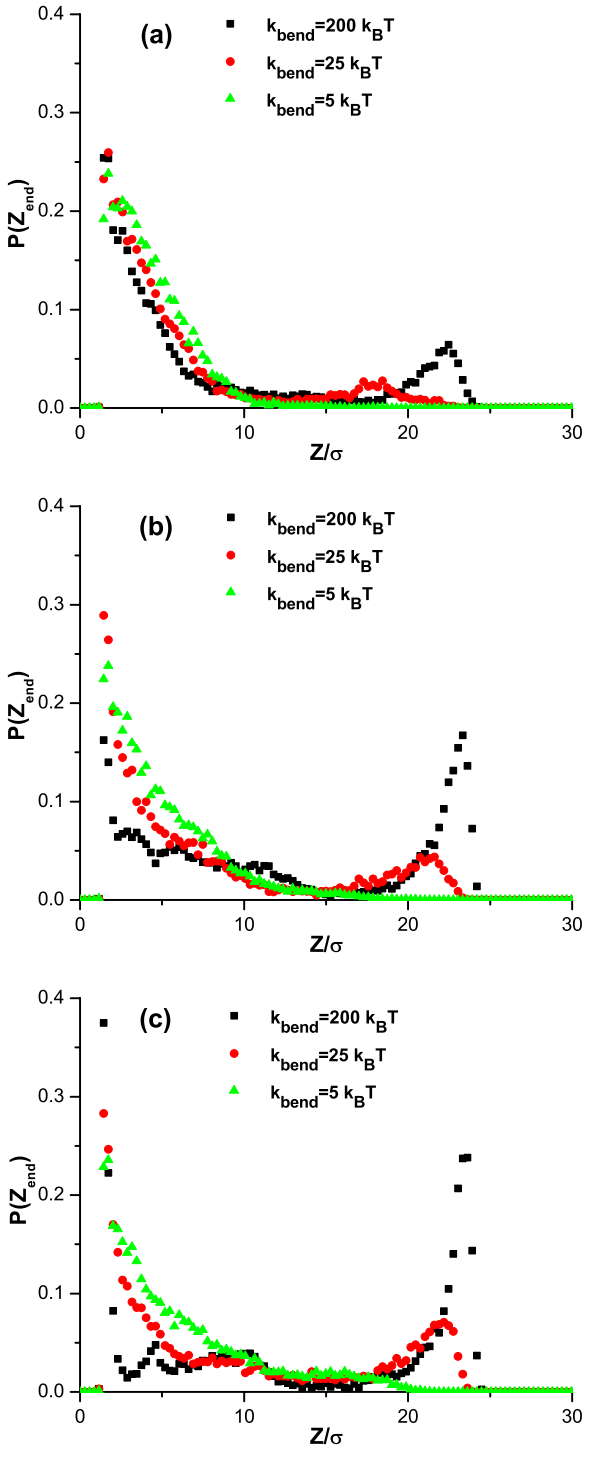

FIG. 4. (Color online) Histogram of the average distance of the end monomers of the chains from the grafting surface for the brushes of flexible, semiflexible and rodlike diblock polyampholytes at grafting densities (a) $\rho_a\sigma^2=0.02$, (b) $\rho_a\sigma^2=0.06$, and (c) $\rho_a\sigma^2=0.10$.

chains. The histograms $P(z_{end})$ in Fig. 4 show that in the brush of flexible chains at all grafting densities the end monomers are mostly distributed near the grafting surface showing that the positive blocks of the chains are mostly turned back toward the anchored negative blocks. The profile of this histogram also doesn't depend noticeably on the grafting density. The histograms $P(z_{end})$ for brushes of semiflexible and rodlike chains show that two maxima appear and their height increase with increasing the grafting density. By combining the information obtained from histograms $P(R)$ and $P(z_{end})$ for the brush of rodlike chains it can be understood that at high grafting densities a fraction of the chains,

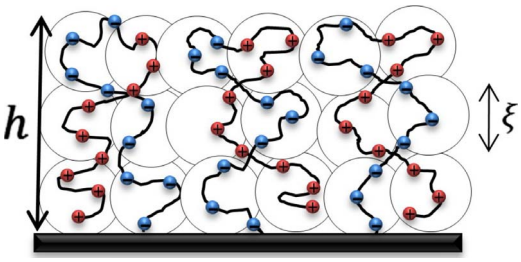

FIG. 5. (Color online) The blob picture of a flexible diblock polyampholyte brush. The blobs of positive charge are more probably surrounded by blobs of negative charge. Positively and negatively charged monomers are shown by red (+) and blue (–) sphere, respectively. The neutral monomers are not shown for clarity. h and ξ are the brush thickness and correlation blob size, respectively.

which are perpendicular to the grafting surface coexist with the remaining fraction which fluctuate in the vicinity of the grafting surface. In the case of the brush of semiflexible chains also, the fraction of perpendicular chains to the brush surface coexist with the chains, which are buckled toward the grafting surface [29]. Histograms $P(R)$ and $P(z_{end})$ show that conformations of the brushes of semiflexible and rodlike chains change noticeably with changing the grafting density despite the case of the brush of flexible chains.

III. LINEAR DEPENDENCE OF THE BRUSH THICKNESS ON THE GRAFTING DENSITY: SCALING APPROACH

As mentioned in the previous section, our MD simulations show that the brush thickness is a linear function of the grafting density regardless of different values of grafted diblock polyampholytes bending energy. Also, as it is shown in Fig. 2, in cases of the brushes of flexible chains the slope of the fitted line to the average thickness versus the grafting density is considerably smaller than that in two other cases. We use here a simple scaling theory similar to that of the solution of charge-symmetric diblock polyampholytes [34] to describe the linear dependence of the brush thickness on the grafting density. This scaling analysis is applicable to the brushes of flexible diblock polyampholytes.

Consider M flexible diblock polyampholyte chains end grafted to a flat surface of area A. The degree of polymerization of each chain and the fraction of charged monomers are N and f, respectively. Electrostatic attractive interactions between oppositely charged blocks of the chains lead them to form a dense layer of positive and negative monomers of average thickness h near the grafting surface (see Fig. 5). Inside the layer, to use the blob concept we define correlation length ξ as a length scale that electrostatic interactions don't perturb the chains statistics at smaller length scales and are dominant over thermal fluctuations at larger length scales. Let suppose that the number of monomers inside the correlation blob is g and we have $\xi \approx bg^{\nu}$ where b and ν are the Kuhn length and the Flory exponent, respectively. Accordingly, the layer is a melt of correlation blobs, in which positive blobs with a high probability are surrounded by negative blobs. Electrostatic interaction between any two neighboring blobs is of the order of the thermal energy, k_BT,

$$k_BT\left|\frac{l_Bf^2g^2}{\xi}\right| \approx k_BT. \tag{6}$$

Thus, we obtain $\xi \approx l_Bf^2g^2 \approx b(\frac{l_Bf^2}{b})^{\nu/(\nu-2)}$. As a result, the local monomer concentration inside the blob is

$$\rho_{local} \approx \frac{g}{\xi^3} \approx \frac{\xi^{(1-3\nu)/\nu}}{b^{1/\nu}} \approx \frac{1}{b^3}\left(\frac{l_Bf^2}{b}\right)^{(1-3\nu)/(\nu-2)}. \tag{7}$$

Considering that correlation blobs are space filling, the global monomer concentration, $\rho_{global}=\frac{MN}{Ah}=\rho_a\frac{N}{h}$, approximately equals to the local monomer concentration, $\rho_{global} \approx \rho_{local}$. Thus, dependence of the thickness of a brush of diblock polyampholytes on the grafting density can be obtained as

$$h \approx \rho_a N b^3\left(\frac{l_B}{b}f^2\right)^{(3\nu-1)/(\nu-2)}. \tag{8}$$

The main prediction of this equation in the range of its validity is as follows. The brush thickness, h, is a linear function of the grafting density, ρ_a, irrespective of the values of the system parameters. Only the slope of this linear function, $\alpha=Nb^3(\frac{l_B}{b}f^2)^{(3\nu-1)/(\nu-2)}$, depends on the values of the system parameters.

One should note here that despite the bulk solution of flexible diblock polyampholytes, in a polyampholyte brush the fact that the chains are end grafted to the surface introduces an additional length scale to the system, namely, $d=\rho_a^{-1/2}$. In the scaling analysis presented here, if the size of the correlation length, ξ, exceeds the separation between the grafting points, d, the scaling approach becomes inconsistent. Although linear dependence of the brush thickness on the grafting density is observed at all values of the bending energy used in our simulations, the condition $\xi < d$ is valid only in the case of the brush of flexible chains with $k_{bend}=0$. In this case the values of $\frac{\xi}{d}$ corresponding to lowest and highest values of the grafting density we have used in our simulations are 0.19 and 0.45, respectively. For the set of parameters used in our simulations, in the case of the brush with $k_{bend}=0$ the upper limit of the validity of the scaling method ($\xi \simeq d$) corresponds to the grafting density $\rho_a\sigma^2 \simeq 0.55$, which is quite far from our range of the grafting density. For a brush of flexible chains with $k_{bend}=0$ using the values $b \simeq \sigma$ and $\nu \simeq \frac{3}{5}$ gives the slope $\alpha_f \simeq 35$ for the brush thickness versus the grafting density for the used set of system parameters. As it is shown in Fig. 2, the value of α_f obtained from our simulations of flexible chains is $\alpha_f \simeq 20.0$, which is in reasonable agreement with prediction of the scaling method.

Our scaling method is not consistently applicable for the brush of flexible chains with $l_p=5\sigma$ because the range of the grafting density used in our simulations is higher than the validity range of the condition $\xi < d$ in this case. This method is not also applicable for the brushes of semiflexible and rodlike chains because in these cases the Kuhn length exceeds the contour length of the chains. The fact that the average thickness linearly depends on the grafting density at all values of k_{bend} used in our simulations shows that al-

though the scaling method presented here cannot be used to describe all the simulation results, this linear dependence persists over a wide range of the system parameters.

IV. CONCLUSIONS AND DISCUSSION

Brushes of flexible, semiflexible, and rodlike diblock polyampholytes have been studied using MD simulations and a scaling analysis has been presented to describe the results of the simulation of flexible chins brush. The average thickness as a function of the grafting density and histograms of equilibrium conformations of the brushes are obtained. Strong dependence of the system conformations on the grafting density and separation of the chains into two coexisting fractions at high grafting densities have been observed in cases of the brushes of semiflexible and rodlike chains. In cases of the brushes of flexible chains, single-chain behavior is dominant and dependence of the brush conformations on the grafting density is very weak. In spite of above mentioned differences, it has been observed that dependence of the average brush thickness on the grafting density is linear for brushes of all different chains. This linear dependence resulted from our MD simulations has been described well using a simple scaling method in the case of the brush of flexible chains.

Brushes of polyelectrolytes and polyampholytes are dense assembly of these macromolecules in which the interplay between electrostatic correlations, strong excluded volume effects and bending elasticity of the chains determine equilibrium properties of the system. The main differences between brushes of polyelectrolyte and polyampholyte chains originates from opposite trends of interchain and intrachain electrostatic interactions and different rules of counterions osmotic pressure in these brushes. In a brush of polyelectrolyte chains, most of counterions are contained inside the brush and their osmotic pressure tends to increase the brush thickness. In a brush of overall neutral polyampholytes, however, counterions are outside the brush and have no effect on the brush thickness. Linear dependence of polyelectrolyte brush thickness on the grafting density has theoretically been described [17–19]. The results of a recent simulation of semiflexible polyampholytes [29] and our simulations and theoretical analysis here show that linear dependence of the average thickness on the grafting density is also the case in the brush of polyampholyte chains. Amount of the flexibility of the chains, which control the strength of excluded volume effects and interchain correlations, causes the equilibrium conformations of the brushes of three different polyampholytes to be different. In brushes of semiflexible and rodlike polyampholytes, strong dependence of the equilibrium conformations on the grafting density and separation of the chains into two coexisting fractions at high grafting densities are resulted from strong electrostatic and excluded volume correlations between the chains. Similar phenomenon has been observed in the brush of rodlike polyelectrolytes [22].

To pay attention to possible finite-size effects in our simulations, we have calculated the average size of the chains lateral fluctuations as well as the histograms $P(z_{end})$ and $P(R)$ for a larger brush containing $M=8\times 8=64$ semiflexible chains at the grafting density $\rho_a\sigma^2=0.1$ [29]. The average size of lateral fluctuations is defined as $\langle l_{lat}\rangle=\frac{1}{M}\Sigma_{i=1}^{M}\langle R_{i\|}\rangle$, where $R_{i\|}=|\mathbf{R}_i-\mathbf{R}_i.\hat{z}|$ and $\langle\ldots\rangle$ denotes averaging over equilibrium configurations. We have found that the histograms $P(R)$ and $P(z_{end})$ do not change noticeably with increasing the system size [29]. Also, we have found that the value of $\langle l_{lat}\rangle$ is smaller than the lateral size, L, of the simulation box of a brush containing $M=25$ chains at the same grafting density. This result shows that in simulation of the brush of $M=25$ polyampholytes, the chains do not overlap with their own images. Accordingly, to avoid time consuming simulations of larger brushes, we concentrated on the simulations of the brushes containing $M=25$ chains.

ACKNOWLEDGMENT

We would like to acknowledge A. Naji for his useful suggestions.

[1] S. Förster and M. Schmidt, Adv. Polym. Sci. **120**, 51 (1995).
[2] J. L. Barrat and J. F. Joanny, Adv. Chem. Phys. **94**, 1 (1996).
[3] A. V. Dobrynin, R. H. Colby, and M. Rubinstein, J. Polym. Sci., Part B: Polym. Phys. **42**, 3513 (2004).
[4] J. Rühe, M. Ballauff, M. Biesalski, P. Dziezok, F. Gröhn, D. Johannsmann, N. Houbenov, N. Hugenberg, R. Konradi, S. Minko, M. Motornov, R. R. Netz, M. Schmidt, C. Seidel, M. Stamm, T. Stephan, D. Usov, and H. Zhang, Adv. Polym. Sci. **165**, 79 (2004).
[5] Y. Hong, R. L. Legge, S. Zhang, and P. Chen, Biomacromolecules **4**, 1433 (2003).
[6] S. Jun, Y. Hong, H. Imamura, B. Y. Ha, J. Bechhoefer, and P. Chen, Biophys. J. **87**, 1249 (2004).
[7] R. Messina, Eur. Phys. J. E **22**, 325 (2007).
[8] C. M. Wijmans and E. B. Zhulina, Macromolecules **26**, 7214 (1993).
[9] E. Lindberg and C. Elvingson, J. Chem. Phys. **114**, 6343 (2001).
[10] J. Klos and T. Pakula, Macromolecules **37**, 8145 (2004).
[11] A. S. Almusallam and D. S. Sholl, Nanotechnology **16**, S409 (2005).
[12] P. Pincus, Macromolecules **24**, 2912 (1991).
[13] E. B. Zhulina and O. V. Borisov, Macromolecules **29**, 2618 (1996).
[14] E. B. Zhulina, J. K. Wolterink, and O. V. Borisov, Macromolecules **33**, 4945 (2000).
[15] E. B. Zhulina, O. V. Borisov, and T. M. Birstein, J. Phys. II **2**, 63 (1992).
[16] E. B. Zhulina and O. V. Borisov, J. Chem. Phys. **107**, 5952 (1997).
[17] A. Naji, R. R. Netz, and C. Seidel, Eur. Phys. J. E **12**, 223 (2003).

[18] H. Ahrens, S. Forster, C. A. Helm, N. A. Kumar, A. Naji, R. R. Netz, and C. Seidel, J. Phys. Chem. B **108**, 16870 (2004).
[19] A. Naji, C. Seidel, and R. R. Netz, Adv. Polym. Sci. **198**, 149 (2006).
[20] F. S. Csajka and C. Seidel, Macromolecules **33**, 2728 (2000).
[21] C. Seidel, Macromolecules **36**, 2536 (2003).
[22] H. Fazli, R. Golestanian, P. L. Hansen, and M. R. Kolahchi, Europhys. Lett. **73**, 429 (2006).
[23] O. V. Borisov, T. M. Birstein, and E. B. Zhulina, J. Phys. II **1**, 521 (1991).
[24] N. P. Shusharina and P. Linse, Eur. Phys. J. E **4**, 399 (2001).
[25] N. P. Shusharina and P. Linse, Eur. Phys. J. E **6**, 147 (2001).
[26] A. Akinchina, N. P. Shusharina, and P. Linse, Langmuir **20**, 10351 (2004).
[27] A. Akinchina and P. Linse, Langmuir **23**, 1465 (2007).
[28] P. Linse, J. Chem. Phys. **126**, 114903 (2007).
[29] M. Baratlo and H. Fazli, Eur. Phys. J. E **29**, 131 (2009).
[30] H. J. Limbach, A. Arnold, B. A. Mann, and C. Holm, Comput. Phys. Commun. **174**, 704 (2006).
[31] G. S. Grest and K. Kremer, Phys. Rev. A **33**, 3628 (1986).
[32] R. Strebel and R. Sperb, Mol. Simul. **27**, 61 (2001).
[33] A. Arnold and C. Holm, Comput. Phys. Commun. **148**, 327 (2002).
[34] N. P. Shusharina, E. B. Zhulina, A. V. Dobrynin, and M. Rubinstein, Macromolecules **38**, 8870 (2005).